Robust Nonlinear Control for Direct Torque Control of Induction Motor Drive Using Space Vector Modulation

S. BELKACEM, F. NACERI, R. ABDESSEMED

LEB, Department of Electrical Engineering, University of Batna, Algeria

Tel : +213 033 92 19 50, Fax : +213 033 51 81 23

E-mail : belkacem_sebti@yahoo.fr

Abstract: *To solve the problems of torque ripple and inconstant switch frequency of inverter in the conventional direct torque control (DTC), a novel DTC method using space vector modulation (SVM) is proposed based on input–output feedback linearization technique, where hysteresis controller is substituted by input–output feedback linearization and switch table is substituted by SVM. In order to preserve the system robustness with respect to rotor resistances variations and uncertainties. IM drive simulation model with novel SVM-DTC is created and studied using MATLAB. Simulation results demonstrate the feasibility and validity of the proposed DTC system by effectively accelerating system response, reducing torque and flux ripple and a very satisfactory performance has been achieved.*

Key words: *input–output feedback linearization, induction motor, SVM, direct torque control, key parameter variation.*

1. Introduction

The direct torque control (DTC) scheme has been increased due to several factors such as quick torque response and robustness against the motor parameter variations [1,2]. The conventional DTC algorithm using the hysteresis based voltage switching method has relative merits of simple structure and easy implementation. The performance of such a scheme depends on the error band set between the desired and measured torque and stator flux values. In addition, in this control scheme, the inverter switching frequency is changed according to the hysteresis bandwidth of flux and torque controllers and the variation of speed and motor parameters. Superior motor performance is achieved by narrower hysteresis bands especially in the high speed region. As a result, this approach will not be suitable for high power drives such as those used in tractions, as they require good torque control performance at considerably lower frequency.

To overcome the drawbacks problems, some researchers have suggested, the DTC scheme using the space vector modulation (SVM) techniques [3-5].
The control scheme in [6] is sensitive to parameters uncertainty, especially to the stator resistance variations and the stability will be affected by parameter variation. To solve this problem, feedback linearization techniques have been applied to the control of nonlinear plants such as robot manipulators, induction motors, PM synchronous motors and synchronous reluctance motor [7-15]. The main objective is to force the speed and torque of an induction motor to follow their reference trajectories. The basic idea is to first transform a nonlinear system into a linear one by a nonlinear feedback, and then use the well-known linear design techniques to complete the controller design. These techniques, however, require the full knowledge of the system parameters and load conditions with the sufficient accuracy. Recently, an adaptive input–output linearization technique, adaptive backstepping, and adaptive sliding mode have been applied to the induction motor drives [16-23]. Although good performance can be obtained.

The contribution of this paper is to describe a robust DTC-SVM method for a torque and flux control of induction motor drive based on input–output feedback linearization technique. The results show that a satisfactory control performance is obtained.

2. The IM model

With the simplifying assumptions relation to the IM, the model of the IM expressed in the stationary ‘‘ αβ ’’ axes reference frame can be expressed by:

$$\begin{aligned}
\frac{d i_{s\alpha}}{dt} &= -\left(\frac{R_s}{\sigma L_s}+\frac{R_r}{\sigma L_r}\right) i_{s\alpha} - \omega_r i_{s\beta} + \frac{R_r}{\sigma L_r L_s}\Phi_{s\alpha} + \frac{\omega_r}{\sigma L_s}\Phi_{s\beta} + \frac{1}{\sigma L_s} V_{s\alpha} \\
\frac{d i_{s\beta}}{dt} &= -\left(\frac{R_s}{\sigma L_s}+\frac{R_r}{\sigma L_r}\right) i_{s\beta} + \omega_r i_{s\alpha} + \frac{R_r}{\sigma L_r L_s}\Phi_{s\beta} - \frac{\omega_r}{\sigma L_s}\Phi_{s\alpha} + \frac{1}{\sigma L_s} V_{s\beta} \\
\frac{d \Phi_{s\alpha}}{dt} &= V_{s\alpha} - R_s i_{s\alpha} \\
\frac{d \Phi_{s\beta}}{dt} &= V_{s\beta} - R_s i_{s\beta}
\end{aligned} \qquad (1)$$

where i_s , Φ_s , V_s , R and L denote stator currents,

stator flux , stator voltage, resistance and inductance, respectively, ω_r denotes the rotor speed and M is the mutual inductance. $\sigma = 1 - \frac{M^2}{L_s L_r}$ is the redefined leakage inductance.

The generated torque of the induction motor can be expressed in terms of stator currents and stator flux linkage as

$$T_e = \frac{3p}{2}(\Phi_{s\alpha} i_{s\beta} - \Phi_{s\beta} i_{s\alpha}) \tag{2}$$

where p is the number of pole pairs.

The mechanical dynamic equation is given by

$$\frac{d\,\omega_m}{dt} = \frac{3p}{2J}(\Phi_{s\alpha} i_{s\beta} - \Phi_{s\beta} i_{s\alpha}) - \frac{T_L}{J} \tag{3}$$

where J and T_L denote the moment of inertia of the motor , the load torque and ω_m is the rotor mechanical speed ($\omega_r = p\omega_m$).

For the proposed nonlinear input-output feedback linearization controller, the state coordinate transformation is applied. Therefore, the state coordinates transformed model from (1) can be rewritten in a compact form as

$$\begin{aligned} \dot{x} &= f(x) + g_1(x).V_{s\alpha} + g_2(x).V_{s\beta} \\ y &= h(x) \end{aligned} \tag{4}$$

where x is defined as:

$$f(x) = \begin{bmatrix} -(\frac{R_s}{\sigma L_s} + \frac{R_r}{\sigma L_r}) i_{s\alpha} - \omega_r i_{s\beta} + \frac{R_r}{\sigma L_r L_s}\Phi_{s\alpha} + \frac{\omega_r}{\sigma L_s}\Phi_{s\beta} \\ -(\frac{R_s}{\sigma L_s} + \frac{R_r}{\sigma L_r}) i_{s\beta} + \omega_r i_{s\alpha} + \frac{R_r}{\sigma L_r L_s}\Phi_{s\beta} - \frac{\omega_r}{\sigma L_s}\Phi_{s\alpha} \\ -R_s i_{s\alpha} \\ -R_s i_{s\beta} \end{bmatrix} \tag{5}$$

$$x = \begin{bmatrix} i_{s\alpha}, i_{s\beta}, \Phi_{s\alpha}, \Phi_{s\beta} \end{bmatrix}^T, \; g_1(x) = \begin{bmatrix} \frac{1}{\sigma L_s} & 0 & 1 & 0 \end{bmatrix}^T$$

$$g_2(x) = \begin{bmatrix} 0 & \frac{1}{\sigma L_s} & 0 & 1 \end{bmatrix}^T \tag{6}$$

At this stage, the generated torque T_e and the squared modules of the stator flux linkage $\left|\Phi_s\right|^2 = {\Phi_{s\alpha}}^2 + {\Phi_{s\beta}}^2$ are assumed to be the system outputs. Therefore, by considering

$$\begin{aligned} h_1(x) &= T_e = \frac{3p}{2}(\Phi_{s\alpha} i_{s\beta} - \Phi_{s\beta} i_{s\alpha}) \\ h_2(x) &= \left|\Phi_s\right|^2 = {\Phi_{s\alpha}}^2 + {\Phi_{s\beta}}^2 \end{aligned} \tag{7}$$

Define the controller objectives y_1 and y_2 as

$$\begin{aligned} y_1 &= h_1(x) \\ y_2 &= h_2(x) \end{aligned} \tag{8}$$

3. Input-output feedback linearization

To linearize the nonlinear model in (4), the controlled variable is differentiated with respect to time until the input appears. This can be easily done by introducing the Lie derivative.

3.1 Lie Derivatives

Consider system (4). Differentiating the output y with respect to time yields:

$$\dot{y} = \frac{\partial h}{\partial x}\dot{x} = \frac{\partial h}{\partial x}\left[f(x) + g(x)V\right] = L_f h(x) + L_g h(x)V \tag{9}$$

where $L_f h(x) = \frac{\partial h}{\partial x} f(x)$, $L_g h(x) = \frac{\partial h}{\partial x} g(x)$

The function $L_f h(x)$ is called the Lie Derivative of $h(x)$ with respect to $f(x)$, and corresponds to the derivative of h along the trajectories of the system $\dot{x} = f(x)$. Similarly, $L_g h(x)$ is called the Lie Derivative of h with respect to g , and corresponds to the derivative of function $h(x)$ along the trajectories of the system $\dot{x} = g(x)$.

3.2 Relative degree of a nonlinear system

For nonlinear systems, the relative degree r of system (4) corresponds to the number of times the output $y = h(x)$ has to be differentiated with respect to time before the input u appears explicitly in the resulting equations.

System (4) is said to have a relative degree $r, 1 \le r \le n$ in R^n if $\forall x \in R^n$:

$$\begin{aligned} &L_g L_f^{i-1} h(x) = 0 \qquad i = 1, 2, ..., r-1 \\ &L_g L_f^{r-1} h(x) \neq 0 \end{aligned} \tag{10}$$

where

$$L_g L_f^i h(x) = L_g\left[L_f^i h(x)\right], L_f^i h(x) = L_f\left[L_f^{i-1} h(x)\right], i = 1, 2, ..., r-1$$

and $L_f^0 h(x) \triangleq h(x)$

Using the above notation, we can obtain that

3.2.1 Relative degree of the torque

$$\begin{aligned} \dot{y}_1 &= L_f h_1(x) + L_{g1} h_1(x) V_{s\alpha} + L_{g2} h_1(x) V_{s\beta} \\ &= \frac{\partial h_1}{\partial x}.f(x) + \frac{\partial h_1}{\partial x} g_1(x).V_{s\alpha} + \frac{\partial h_1}{\partial x} g_2(x).V_{s\beta} \end{aligned} \tag{11}$$

with

$$L_f h_1 = -\frac{3p}{2}\Phi_{s\beta}\left[-(\frac{R_s}{\sigma L_s}+\frac{R_r}{\sigma L_r})i_{s\alpha} - \omega_r i_{s\beta} + \frac{\omega_r}{\sigma L_s}\Phi_{s\beta}\right] + \frac{3p}{2}\Phi_{s\alpha}\left[-(\frac{R_s}{\sigma L_s}+\frac{R_r}{\sigma L_r})i_{s\beta} + \omega_r i_{s\alpha} - \frac{\omega_r}{\sigma L_s}\Phi_{s\alpha}\right]$$

$$L_{g1} h_1 = \frac{3p}{2}(i_{s\beta} - \frac{1}{L_s\sigma}\Phi_{s\beta})$$

$$L_{g2} h_1 = \frac{3p}{2}\left(\frac{1}{L_s\sigma}\Phi_{s\alpha} - i_{s\alpha}\right)$$

The relative degree of $y_1(x)$ is $r_1 = 1$.

3.2.2 Relative degree of the flux

$$\begin{aligned}\dot{y}_2 &= L_f h_2(x) + L_{g1} h_2(x) V_{s\beta} + L_{g2} h_2(x) V_{s\alpha} \\ &= \frac{\partial h_2}{\partial x}.f(x) + \frac{\partial h_2}{\partial x} g_1(x).V_{s\alpha} + \frac{\partial h_2}{\partial x} g_2(x).V_{s\beta}\end{aligned} \quad (12)$$

with

$$L_f h_2 = -2R_s\left(\Phi_{s\alpha} i_{s\alpha} - \Phi_{s\beta} i_{s\beta}\right)$$

$$L_{g1} h_2 = 2\Phi_{s\alpha}$$

$$L_{g2} h_2 = 2\Phi_{s\beta}$$

The relative degree of $y_2(x)$ is $r_2 = 1$

3.2.3 Relative degree of the system

The total degree of the system is equal to order N($r = r_1 + r_2 = N = 2$). The system is exactly linearizable.

4. Decoupling matrix

The matrix defining the relation between the physical input (u) and the output derivative (y(x)) is given by the expression (13).

$$\begin{bmatrix}\dot{y}_1 \\ \dot{y}_2\end{bmatrix} = A(x) + E(x)\begin{bmatrix}V_{s\alpha} \\ V_{s\beta}\end{bmatrix} \quad (13)$$

with

$$A(x) = \begin{bmatrix}L_f h_1 \\ L_f h_2\end{bmatrix}$$

$$E(x) = \begin{bmatrix}L_{g1} h_1 & L_{g2} h_1 \\ L_{g1} h_2 & L_{g2} h_2\end{bmatrix}$$

$$E(x) = \begin{bmatrix}\frac{3p}{2}(i_{s\beta} - \frac{1}{L_s\sigma}\Phi_{s\beta}) & \frac{3p}{2}\left(\frac{1}{L_s\sigma}\Phi_{s\alpha} - i_{s\alpha}\right) \\ 2\Phi_{s\alpha} & 2\Phi_{s\beta}\end{bmatrix} \quad (14)$$

$$\det(E) = \frac{3p}{2}(i_{s\beta} - \frac{1}{L_s\sigma}\Phi_{s\beta}).2\Phi_{s\beta} - \frac{3p}{2}\left(\frac{1}{L_s\sigma}\Phi_{s\alpha} - i_{s\alpha}\right).2\Phi_{s\alpha}$$

$$= 3p(i_{s\beta} - \frac{1}{L_s\sigma}\Phi_{s\beta}).\Phi_{s\beta} - 3p\left(\frac{1}{L_s\sigma}\Phi_{s\alpha} - i_{s\alpha}\right).\Phi_{s\alpha}$$

$$\det(E) = 3p\left[-\frac{1}{L_s\sigma}(\Phi_{s\beta}^2 + \Phi_{s\alpha}^2) + i_{s\beta}\Phi_{s\beta} + i_{s\alpha}\Phi_{s\alpha}\right] \quad (15)$$

using the induction motor model of (1)

$$\begin{aligned}i_{s\alpha} &= \frac{1}{\sigma L_s}\Phi_{s\alpha} - \frac{M}{\sigma L_s L_r}\Phi_{r\alpha} \\ i_{s\beta} &= \frac{1}{\sigma L_s}\Phi_{s\beta} - \frac{M}{\sigma L_s L_r}\Phi_{r\beta}\end{aligned} \quad (16)$$

Linking (15) and (16)

$$\det(E) = -3p.\frac{M}{\sigma L_s L_r}\left[\Phi_{s\beta}\Phi_{r\beta} + \Phi_{s\alpha}\Phi_{r\alpha}\right] \quad (17)$$

It is clear that the matrix E(x) is always reversible, the product of stator flux and rotor flux can not be equal to zero the following input-output feedback linearization is introduced for the system shown in (4)

$$\begin{bmatrix}V_{s\alpha} \\ V_{s\beta}\end{bmatrix} = E^{-1}(x)\left[-A(x) + \begin{bmatrix}V_1 \\ V_2\end{bmatrix}\right] \quad (18)$$

where

$V = \begin{bmatrix}V_1 \\ V_2\end{bmatrix}$ are the new inputs.

substituting (18) in (13) ,the system dynamic are

$$\begin{cases}V_1 = \dot{h}_1(x) \\ V_2 = \dot{h}_2(x)\end{cases} \quad (19)$$

To ensure a perfect regulation and track the desired signals of the flux and torque towards their reference, V_1 , V_2 are chosen as follows:

$$\begin{cases}V_1 = \left|\dot{\Phi}_s\right|_{ref}^2 + k_1\left(\left|\Phi_s\right|_{ref}^2 - \left|\Phi_s\right|^2\right) \\ V_2 = \dot{T}_{e\,ref} + k_2(T_{e\,ref} - T_e)\end{cases} \quad (20)$$

where subscript 'ref' denotes the reference value. (k_1 , k_2) are constant design parameters to be determined in order to make the decoupled system (20) stable. The behavior of the linearized model is imposed by the poles placement methods. Theses coefficients are selected such as the equation $s + k_1$, $s + k_2$ are the polynomials of Hurwitz.

5. Voltage space vector modulation

The voltage vectors, produced by a 3-phase PWM inverter, divide the space vector plane into six sectors as shown in Fig. 1

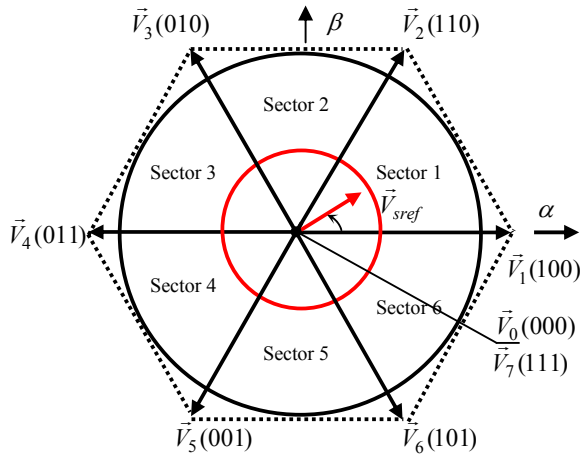

Fig. 1. The diagram of voltage space vectors

In every sector, each voltage vector is synthesized by basic space voltage vector of the two side of sector and one zero vector. For example, in the first sector, $\bar{V}_{s\,ref}$ is a synthesized voltage space vector and expressed by:

$$\bar{V}_{s\,ref}T_s = \bar{V}_0T_0 + \bar{V}_1T_1 + \bar{V}_2T_2 \tag{21}$$

$$T_s = T_0 + T_1 + T_2 \tag{22}$$

where, T_0, T_1 and T_2 is the work time of basic space voltage vectors $\bar{V}_0$, $\bar{V}_1$ and $\bar{V}_2$ respectively.

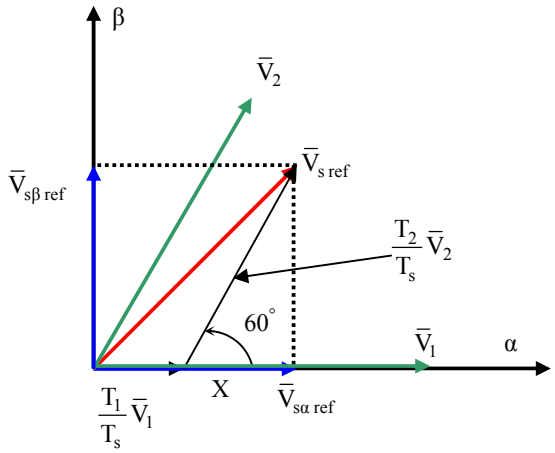

Fig. 2. Projection of the reference voltage vector

The determination of the amount of times T_1 and T_2 is given by simple projections:

$$T_1 = \frac{T_s}{2E}\left(\sqrt{6}.V_{s\beta\,ref} - \sqrt{2}.V_{s\alpha\,ref}\right) \tag{23}$$

$$T_2 = \sqrt{2}\frac{T_s}{E}V_{s\beta\,ref} \tag{24}$$

The rest of the period spent in applying the null-vector. For every sector, commutation duration is calculated. The amount of times of vector application can all be related to the following variables:

$$X = \frac{T_s}{E}\sqrt{2}.V_{s\beta\,ref} \tag{25}$$

$$Y = \frac{T_s}{E}\left(\frac{\sqrt{2}}{2}.V_{s\beta\,ref} + \frac{\sqrt{6}}{2}.V_{s\alpha\,ref}\right) \tag{26}$$

$$Z = \frac{T_s}{E}\left(\frac{\sqrt{2}}{2}.V_{s\beta\,ref} - \frac{\sqrt{6}}{2}.V_{s\alpha\,ref}\right) \tag{27}$$

The application durations of the sector boundary vectors are tabulated as follows:

Table 1. Durations of the sector boundary vectors

Sector	1	2	3	4	5	6
T_1	Z	Y	-Z	-X	X	-Y
T_2	Y	-X	X	Z	-Y	-Z

The third step is to compute the three necessary duty cycles as;

$$T_{aon} = \frac{T_s - T_1 - T_2}{2} \tag{28}$$

$$T_{bon} = T_{aon} + T_1 \tag{29}$$

$$T_{con} = T_{bon} + T_2 \tag{30}$$

The last step is to assign the right duty cycle (T_{xon}) to the right motor phase according to the sector.

Table 2. Cycles of the PWM outputs.

Sector	1	2	3	4	5	6
S_a	T_{bon}	T_{aon}	T_{aon}	T_{con}	T_{bon}	T_{con}
S_b	T_{aon}	T_{con}	T_{bon}	T_{bon}	T_{con}	T_{aon}
S_c	T_{con}	T_{bon}	T_{con}	T_{aon}	T_{aon}	T_{bon}

6. Sensitivity study and simulation results

In this section, the effectiveness of the proposed algorithm for torque and flux control of an induction motor is verified by computer simulations. The specifications for the used induction motor are listed in table (3). The block scheme of the investigated direct torque control with space vector modulation (DTC-SVM) for a voltage source inverter fed IM is presented in (Fig. 3).

A series of tests were conducted to check the performance of the proposed DTC-SVM. In all sketched figures, the time axis is scaled in seconds.

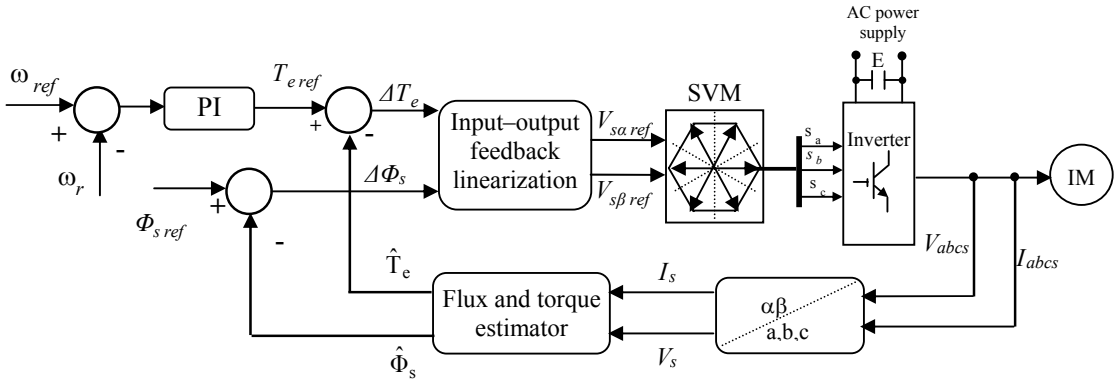

Fig. 3. Block diagram of the proposed DTC-SVM based input–output feedback linearization.

6.1 Speed reversal from 100 rad/sec to -100 rad/sec

The motor reference speed is changed from 100 rad/s to -100 rad/sec at 0.5s and then again, speed is set to 100 rad/s at 1 s. without any change in parameters during the operating time. The performance of the proposed controller for such kind of speed reference is shown in Fig. 4. Plots the reference speed and, actual motor speed with respect to time. It is observed that the actual motor speed follow the reference with good accuracy.

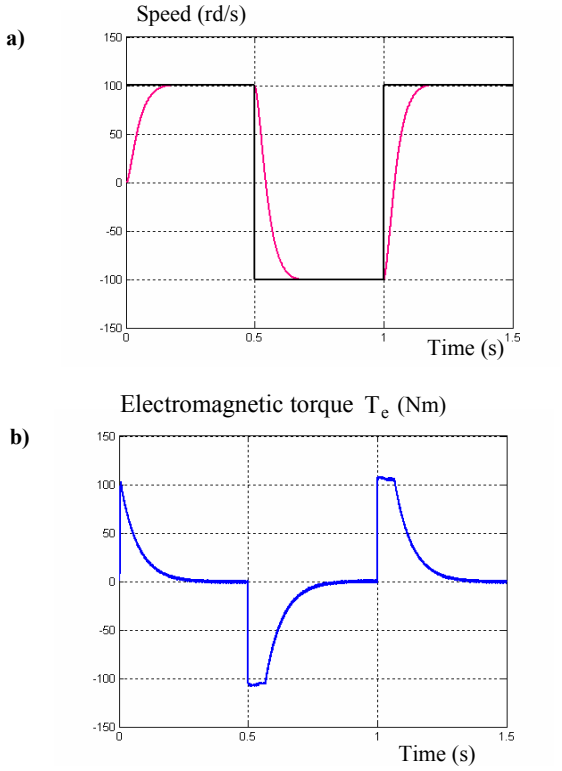

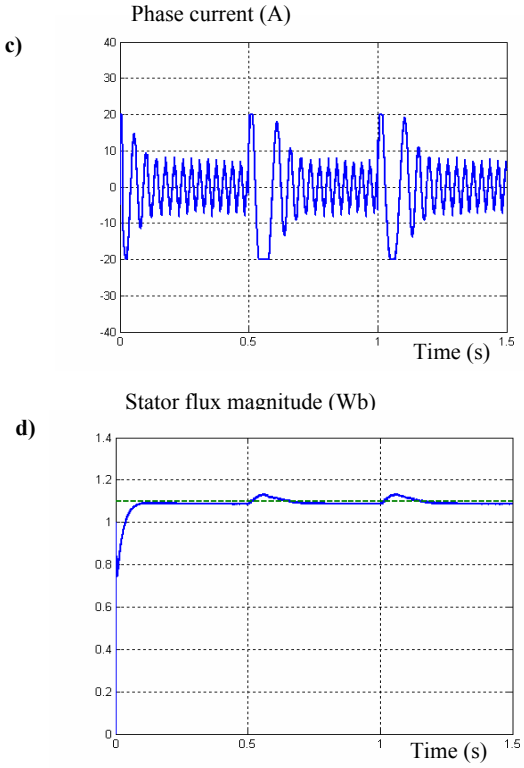

Fig. 4. Simulation results for speed reversal under no parameters change: (**a**) reference and actual rotor speed (**b**) Electromagnetic torque, (**c**) phase current, (**d**) stator flux magnitude.

6.2 Variation of the load torques.

Fig. 5 depicts the simulation results after the introduction of load torque of 10 Nm between 0.5 s and 1s after a leadless starting. We can see the insensibility of the control algorithm to load torque variation and the stator flux responses are not affected by this perturbation.

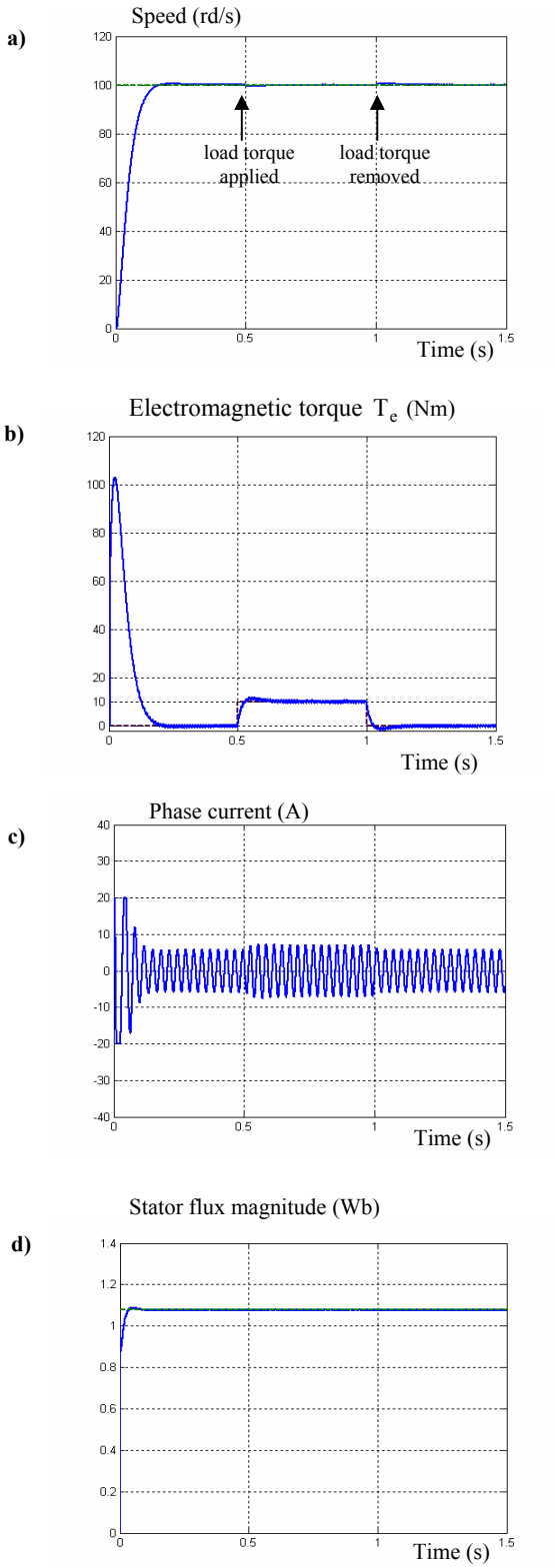

Fig.5. Drive response under load torque change. (**a**) reference and actual rotor speed, (**b**) eelectromagnetic torque, (**c**) phase current, (**d**) stator flux magnitude.

6.3 Variation in the rotor resistance

These tests investigate the influence of the electrical parameters change on the drive performance. Fig. 6 depicts the drive performance for brusque changes in the rotor resistance. it can be seen that the impact of the electrical parameters change on the drive performance is more important. However, those results shown also that the drive robustness and rejection of the perturbations is significantly enhanced.

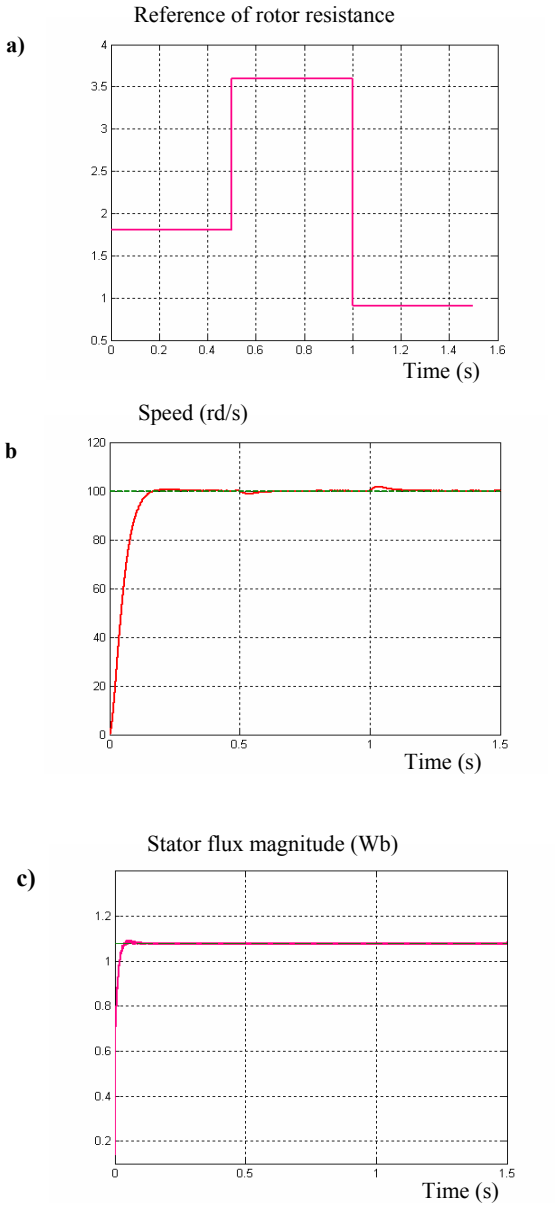

Fig. 6. Drive response under rotor resistance change: (**a**) reference, (**b**) reference and actual rotor speed, (**c**), stator flux magnitude

6.4 Drive response under flux-weakening

This test concerns the drive dynamic under flux-weakening operating. As depicted in Fig. 7, the flux and speed are not affected by the reference flux reduction. Phase current ripple has also a notable reduction.

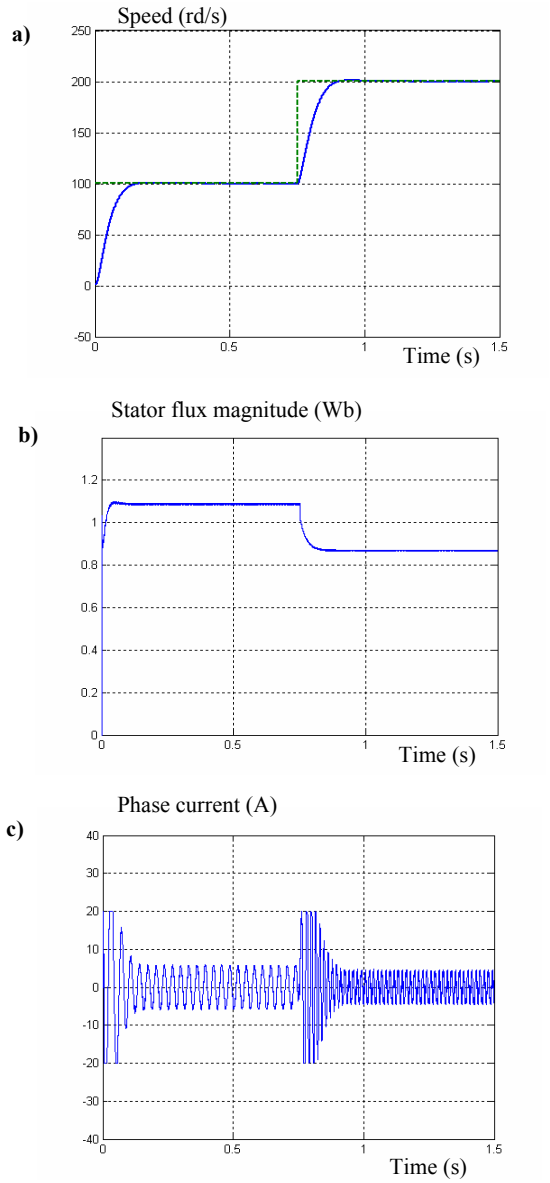

Fig.7. Drive response under flux-weakening. (**a**) Reference and actual rotor speed (**b**) stator flux magnitude, (**a**) phase current

6. 5 Variation in the inertia coefficient.

Fig. 8 shows the drive dynamic under different values of inertia with constant speed reference. It is clear that the speed tracking is little affected by those changes.

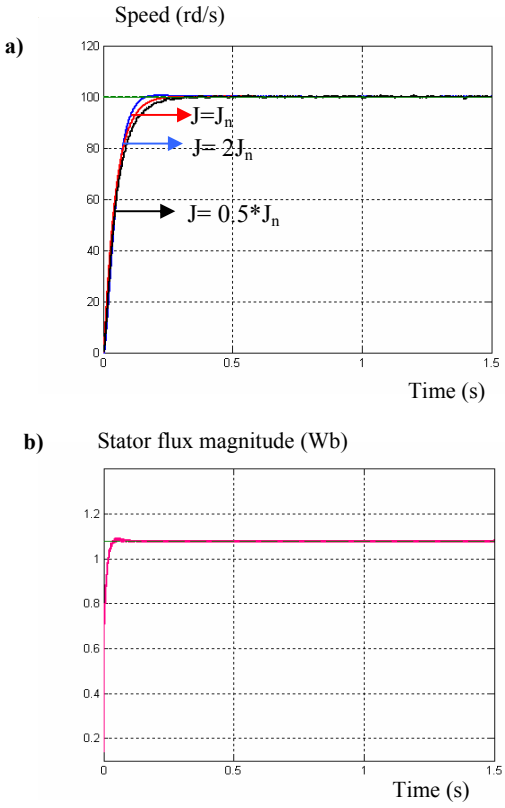

Fig. 8. Drive response under different inertia values. (**a**) Reference and actual rotor speed (**b**) stator flux magnitude.

7. Conclusion

In this paper, we present a robust direct torque control method for voltage inverter – fed induction motor based on a space vector modulation (SVM) scheme combined with input–output feedback linearization technique.

The overall speed and flux control system was verified to be robust to the variations of motor mechanical and electrical parameters variations. Simulation studies were used to demonstrate the characteristics of the proposed method. It is shown that the proposed controller has better tracking performance and robustness against parameters variations as compared with the conventional direct torque control.

Appendix

Table 3

Induction motor parameters

Rated power	4 KW
Pole pair	P= 2
Nominal speed	1440 rpm
Stator inductance	0.1554 H
Rotor inductance	0.1568 H
Mutual inductance	0.15 H
Stator resistance	1.2 Ω
Rotor resistance	1.8 Ω
Machine inertia	0.07 $kg.m^2$
Viscous coefficient	0.00031 $kg.m^2/s$
Rated frequency	50 Hz
Reference flux	$\Phi_{s\,ref}$ =1.1 Wb

References

1. Takahashi I., Ohmori Y.: *High-performance direct torque control of induction motor*. In: IEEE Trans Ind. Appl, Vol. 25(2) 1989, p. 257–264.
2. Casadei D., Profumo F., Serra G., Tani A.: *FOC and DTC: two viable schemes for induction motors torque control*. In: IEEE Trans Power Electron, Vol. 17(5), 2002, p. 779–787.
3. Arab Markadeh G., Soltani R.J.: *Robust direct torque and flux control of adjustable speed sensorless induction machine drive based on space vector modulation using a PI predictive controller*. In: Electrical Engineering, Vol. 88, 2006, p. 485–496.
4. Belkacem S., Naceri F., Abdessemed R.: *Improvement in DTC-SVM of AC Drives Using a New Robust Adaptive Control Algorithm*. In: the international conference on automatic control, December, 20-22, 2009 Hammamet, Tunisia. p. 751–765.
5. Swierczyn'ski D., Kazmierkonwski M.P.: *Direct torque control of permanent magnet synchronous motor (PMSM) using space vector modulation (DTC-SVM) simulation and experimental results*. In: IECON02, 2002, p. 751–755.
6. Lai YS., Chen J. H.: *A new approach to direct torque control of induction motor for constant inverter switching frequency and torque ripple reduction*. In: IEEE Trans Energy Conver, Vol. 6, 2001, p.220–227.
7. Slotine J. J. E. and Li W.: *Applied Nonlinear Control*. Englewood Cliffs, NJ: Prentice-Hall, 1991.
8. Isidori, Z A. *'Nonlinear Control Systems'*, Springer-Verlag. New York, 2nd Ed, 1989.
9. Franklin G. F., Powell J. D., Emami-Naeini A.: *Feedback Control of Dynamic Systems*. In: Reading, MA: Addison-Wesley, 1994.
10. Pereira L. A., Hemerly E. M.: *Design of an adaptive linearizing control for induction motors*. In: Conf. Rec. IEEE IECON'95, 1995, p.1012–1016.
11. Krstic, M., Kanellakopoulos I., Kokotovic P.: *Nonlinear and Adaptive Control Design* New York, Wiley, 1995.
12. Le Pioufle B. :*Comparison of speed nonlinear control strategies for the synchronous servomotor*. In: Elect. Mach. Power Syst., vol. 21, p.151–169, 1993.
13. Luca De A. ,Ulivi G.: *Design of an exact nonlinear controller for induction motors*. In: IEEE Trans. On Automatic Control, 34, 1989, p. 1304-1307.
14. Chiasson J.: *Dynamic feedback linearization of induction motors*. In: IEEE Trans. On Automatic Control, 38, 1993, p.1588-1594
15. Kim K. H., Baik I. C., Chung S. K., and Youn M. J.: *Robust speed control of brushless DC motor using adaptive input–output linearization technique*. In: Proc. IEE—Elect. Power Applica*t*. vol. 144, no. 6, p. 469–475, 1997.
16. Marino R., Peresada S. and Valigi P.: *Adaptive input-output linearizing control of induction motors*. In: IEEE Trans. On Automatic Control, Vol .38, 1993, p. 208-221.
17. Marino R., Peresada S., Tomei P.: *Global adaptive output feedback control of induction motors with uncertain rotor resistance*. In: IEEE Trans. on Automatic Control, Vol .44, 1999, p. 967-983.
18. Dawson Hu J., Qu Z D. M. : *Adaptive tracking control of an induction motor with robustness to parametric uncertainty*. In: Proc Inst Elect Eng – Elect Power App 1994, p. 85–94.
19. Pereira L.A., Hemerly E. M.: *Design of an adaptive linearizing control for induction motors*. In: Conf. Rec. IEEE IECON'95, 1995, p. 1012–1016.
20. Abootorabi Z.G.h., Arab Markadeh R., Soltani J.: *Direct Torque Control of Synchronous Reluctance Motor using Feedback Linearization Including Saturation and Iron Losses*. In: Epe journal, Vol .19, no. 3, 2009.
21. Masood H., Jafar S., Gholamreza A. M., Saeed H.: *Input-Output Feedback Linearization of Sensorless IM Drives with Stator and Rotor Resistances Estimation*. In: Journal of Power Electronics, vol. 9, 2009, p. 654-666.
22. Behzad M. D., Amir F. P., Mohammad N. H., Seung K.: *Design of an Adaptive Backstepping Controller for Doubly Fed Induction Machine Drives*. In: Journal of Power Electronics, vol. 9, no. 3, 2009, p. 343-353,
23. Soltani J., Arab Markadeh G. R.: *A Current-Based Output Feedback Sliding Mode Control for Speed Sensorless Induction Machine Drive Using Adaptive sliding Mode Flux Observer*. In: IEEE 2003, p. 226 231.